ARTICLE

Theoretical Study on Molecular Structures of Methylaluminoxane Nanotubes

Yan-hua Wang[a*], Xiao-wei Wang[b], Jian-ying Tong[a], Jing-cheng Xu[c*]

a. Zhejiang Shuren University, College of Biology and Environmental Engineering, Hangzhou 310015, China
b. Zhejiang Provincial Special Equipment Inspection and Research Institute, Hangzhou 310015, China
c. School of Materials Science and Engineering, University of Shanghai for Science and Technology, Shanghai 200093, China

(Dated: Received on December 25, 2014; Accepted on March 16, 2015)

Density functional theory was used to optimize structures of different methylaluminoxane nanotubes with general formula $[(AlOMe)_2]_n$, $[(AlOMe)_3]_n$ and $[(AlOMe)_4]_n$ cycle unit, where n ranges from 1 to 10. To explore the stability of nanotubes, the binding energies and total energies are calculated. The results indicate that $[(AlOMe)_3]_n$ and $[(AlOMe)_4]_n$ have the stable structure of nanotubes. When n is 3, they have the most stable structure in all systems. Moreover, $[(Al_5O_5)]_n$ and $[(Al_7O_7)]_n$ are also considered, but their dimers have irregular and distorted structures. So $[(Al_5O_5)]_n$ and $[(Al_7O_7)]_n$ nanotubes are impossible to exist.

Key words: Methylaluminoxane, Nanotubes, Density functional theory

I. INTRODUCTION

In 1980, Sinn and Kaminsky discovered that the addition of water to systems such as $Cp_2ZrMe_2/AlMe_3$ caused this rather inactive reaction system to become highly active in ethane polymerization [1]. With these highly active new homogeneous systems, it is possible to fine tune the product polymer polydispersity and microstructure, solely by modifying the organic ligands around the group IV metal [2−7]. It was suspected that partial hydrolysis of $AlMe_3$ brought about the formation of methylaluminoxane (MAO). MAO was prepared by controlled hydrolysis of $AlMe_3$, the complex product solution, which contains MAO together with free and associated $AlMe_3$, acts as a cocatalyst in the process. The exact structure of the MAO is unknown, which has caused a substantial barrier to the understanding of the polymerization process. It was suggested that MAO contained linear chains, cycles, and cagelike clusters, consisting of approximately 5−20 Al−O−Me units [8, 9]. Sinn [10] and Barron *et al.* [11, 12] suggested that cage structures were the most plausible. Since then intense experimental research on the structure and function of MAO has been performed, however there is still not a definite consensus on either topic.

The structure of MAO was difficult to determine in experiment due to its complex system. The characterization of MAO by NMR spectroscopy has been hindered by disproportionation reactions at high temperature and association in solution yielding a mixture of different oligomers with multiple equilibria. Moreover, a structure determination can't be carried out using X-ray diffraction due to the fact that it is not possible to isolate crystalline samples. Without a structural model for MAO, it is nearly impossible to determine the nature of the dormant and active species in polymerization and therefore to understand the function of MAO [13]. Pasynkiewicz has successfully crystallized cage-like tert-butyl analogues of MAO [14]. An extensive computational study by Ziegler *et al.* has shown that $AlMe_3$-free MAO should consist of a mixture of cages of variable size, of which $(AlOMe)_{12}$ is the most abundant [15]. Zakharov and co-workers performed computational studies on a number of pure MAO cages, which are referred to as classic MAO [16−18].

It is possible to theoretically study MAO [19−21] and better understand the structure and function of MAO. Simulations will be able to employ larger (and therefore more realistic) MAO models and to use higher-level methods to determine the accuracy of results obtained with DFT. In this work, we theoretically demonstrate how the alumina nanotubes can be built. The nanotubes are derived from cycles. We illustrate a variety of molecular structures applicable for nanotubes consisting of AlOMe unit, and determine the stability rules for $(AlOMe)_n$ nanotubes.

II. COMPUTATIONAL DETAILS

The density functional theory calculations were carried out using the Dmol^3 software in the Materials

*Authors to whom correspondence should be addressed. E-mail: wwyhss@163.com, jchxu@usst.edu.cn

Studio package [22, 23]. We use the generalized gradient approximation (GGA) with the BLYP [24, 25] exchange correlation functional in the geometry optimization procedure. The nanostructures had not any symmetry constraints and were fully optimized; the criteria of convergences of energy, force, and displacement are set as 10^{-5} Ha, 0.002 Ha/Å, and 0.005 Å, respectively. The binding energy was also calculated. The optimized structures of MAO nanotube are presented in the supplementary material.

III. RESULTS AND DISCUSSION

A. Energetics of nanotube structures

The determination of the structure of MAO can be linked to alumoxanes in general. Alumoxanes are intermediates in the hydrolysis of organoaluminum compounds to aluminum hydroxides. Barron and coworkers [11, 12] suggested that MAO had a three-dimensional cage structure. Within these cage structures four-coordinate aluminum centers bridged by threecoordinate oxygen atoms were thought to predominate. Despite the fact that MAO consists of three-dimensional cage structures, a preliminary investigation on the relative stability of nanotube structures ought to be performed [8, 9]. We decide which subset of structures ought to be studied in depth. In this work, the nanotube structures were constructed by the cyclic chain structure (Fig.1) layer by layer which was composed of alternating three-coordinate aluminum and two-coordinate oxygen atoms [26]. The aluminum and oxygen atoms were connected each other between layers in nanotube (Fig.2). Within these nanotube structures four-coordinate aluminum centers bridged by three-coordinate oxygen atoms were thought to predominate [11]. The four-, six- or eight-membered rings were reasonable in the structure of MAO, but these resulted in structures whose chemical formula substantially deviated from the generally accepted formula of "pure" MAO, $(MeAlO)_n$, where n is an integer. We shall show how the MAO nanotubes can be derived from the cyclic chain structures in Fig.2. For simplicity, we study the formation of nanotubes from the smallest $(AlOMe)_2$, $(AlOMe)_3$ and $(AlOMe)_4$ cycle unit. Larger nanotubes could be derived in a similar way. Depending on the number of added $[(AlOMe)_2]_n$, $[(AlOMe)_3]_n$ and $[(AlOMe)_4]_n$, the MAO nanotubes grow in the length. In our study, n is limited to 1−10.

First of all, it must be noted that during the geometry optimization of the nanotube structure the bonds corresponding to five coordinate Al and four coordinate O atoms broke giving simply a nanotube structure. This shows that such structures are unstable alternatives for MAO. It gives the energy which is gained per monomer when a certain geometry is formed from different monomers. The lower the binding energy per monomer, the more stable the given structure is. Table I gives the binding energies per monomer unit for nanotube structures. Figure 2 shows the $(AlOMe)_2$ unit grows to nanotube. When n is 2, it forms the cube, but its binding energy is nearly zero, which indicates this structure is unstable. Moreover, when n is 3, it has big bonding energy, but its structure change the six remember ring in side view. The square in the middle become rectangle. So $(AlOMe)_2$ unit can't grow to the nanotube, $(AlOMe)_3$ and $(AlOMe)_4$ have been explored. When n ranges between 1 and 10, $[(AlOMe)_3]_n$ and $[(AlOMe)_4]_n$ were determined via DFT level calculations. The binding energies of 23 different nanotubes are shown in Table I, which indicates all of the nanotubes have stable structure because they have big binding energy. The binding energies of $[(AlOMe)_3]_3$ and $[(AlOMe)_4]_3$ have the biggest value in the research system. So n=3, the nanotube is the most stable, the binding energy is nearly a constant value when n is 4−10. Their binding energies are about −78.70 and −104.96 eV, respectively. It indicates they all have the stable structures in more units due to the formation of π conjugated system.

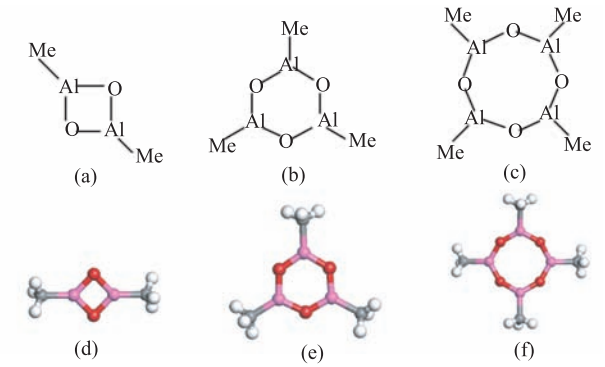

FIG. 1 MAO unit of the cyclic chain structure. (a, d) $(AlOMe)_2$, (b, e) $(AlOMe)_3$, and (c, f) $(AlOMe)_4$.

TABLE I Binding energies for MAO nanotubes.

	E/(kcal/mol)		
n	$[(AlOMe)_2]_n$	$[(AlOMe)_3]_n$	$[(AlOMe)_4]_n$
1	49.5635	76.5030	102.3816
2	0.0001	78.6030	104.6976
3	52.4054	78.7459	105.1771
4		78.6791	104.9519
5		78.6936	104.9552
6		78.7021	104.9615
7		78.7106	104.9682
8		78.7156	104.9711
9		78.7183	104.9739
10		78.7210	104.9758

DOI:10.1063/1674-0068/28/cjcp1412219

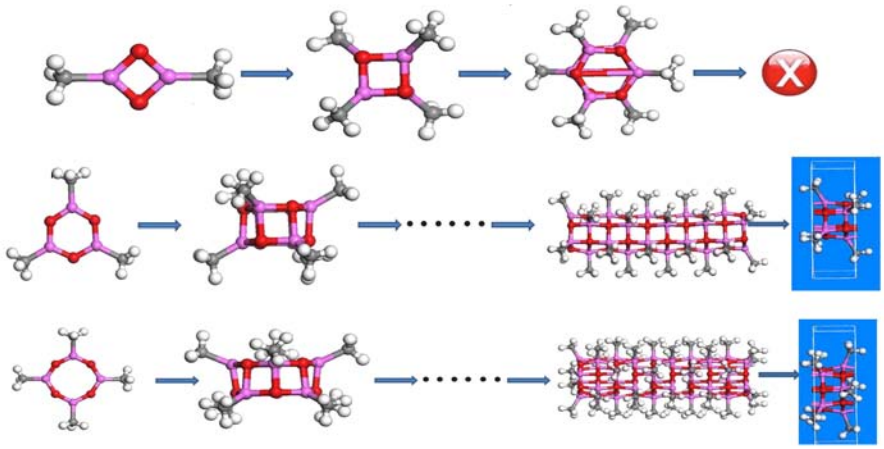

FIG. 2 The growing process of MAO nanotube.

B. Energetic considerations

The total energies of 20 different nanotube structures-$[(AlOMe)_3]_n$ and $[(AlOMe)_4]_n$, where n ranges between 1 and 10, were determined via DFT level calculations. The optimized energies are shown in Fig.3. It was determined that the stability of a given MAO is heavily dependent upon the number of the repeating units. Relative stabilities were estimated by considering the structures in the form $[(AlOMe)_3]_n$ or $[(AlOMe)_4]_n$ and dividing the total energy of the system by n. Such procedure allows the comparison between structures of various sizes by providing the energy/MAO chain cycle unit. The single cyclic chain structure has clearly the lowest stability, which originates from the electron deficiency of aluminum. So MAO cycles incline to aggregate each other, nanotubes assemble by using layer by layer MAO cycles. The structure gets more stable as units grow. When n is 3, energies of $[(AlOMe)_3]_3$ or $[(AlOMe)_4]_3$ are the lowest, both of them have the most stable structure. The energies reach a constant value when the units go on growing. It indicates the nanotubes of $[(AlOMe)_3]_n$ and $[(AlOMe)_4]_n$ have the stable structure. The result is consistent with the binding energies. The highest occupied molecular orbital (HOMO) and the lowest unoccupied molecular orbital (LUMO) are calculated in $[(AlOMe)_3]_2$ or $[(AlOMe)_4]_2$ in order to explore their molecular orbital. Figure 4 shows HOMO is localized, while LUMO is the delocalization of π orbital, which is due to π-electron donation from the lone pairs of oxygen to the vacant p-orbital of aluminum.

C. Structures of MAO nanotubes

The geometries of MAO nanotubes derived from the cyclic chain structure were optimized to evaluate the performance of the methods as well as to determine the preferred structural characteristics. The average distance between the cyclic structures in the 10 units and the period system are shown in Fig.5. It indicates the distance is bigger in the middle of nanotube, and smaller in both ends. The structure parameters in the period system are consistent with the middle of the MAO nanotube. The distances in the middle of the nanotubes are close to a constant value, because five-coordinate aluminum centers are bridged by four-coordinate oxygen atoms in the middle, while four-coordinate aluminum centers are bridged by three-coordinate oxygen atoms in the end of the nanotube. The bonding energies of Al−O in the end of the nanotubes are the strongest in the systems, due to unsaturated aluminum and oxygen atoms. Bond distances and bond angles of MAO nanotubes in different location are listed in Table II.

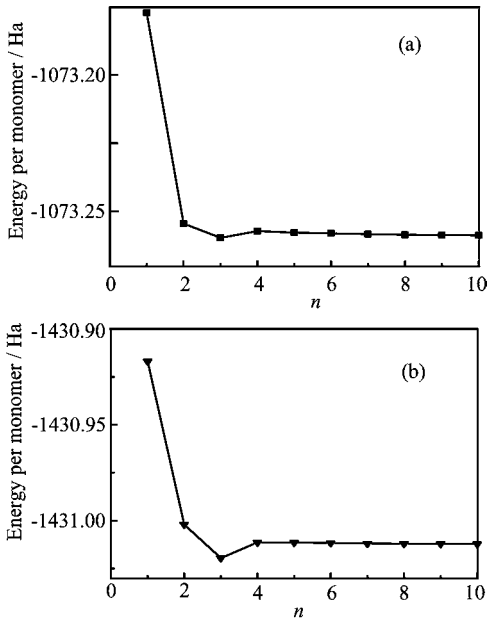

FIG. 3 Energy per monomer *vs.* n of (a) $[(AlOMe)_3]_n$ and (b) $[(AlOMe)_4]_n$.

DOI:10.1063/1674-0068/28/cjcp1412219

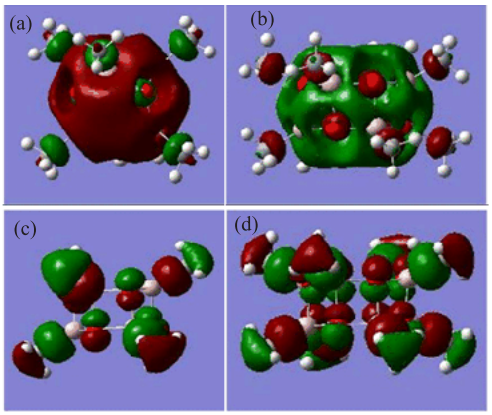

FIG. 4 The LUMO and HOMO of (a, c) $[(AlOMe)_3]_2$ and (b, d) $[(AlOMe)_4]_2$.

TABLE II Bond distances and bond angles of MAO Nanotubes.

	Single	End	Middle	Period[a]
$[(AlOMe)_3]_n$				
Al−O/Å	1.738	1.802	1.874	1.812
Al−O−Al/(°)	125.068	129.998	135.645	130.586
O−Al−O/(°)	114.956	109.699	104.0116	108.693
Al−C/Å	1.96	1.951	1.964	1.962
$[(AlOMe)_4]_n$				
Al−O/Å	1.723	1.785	1.852	1.793
Al−O−Al/(°)	148.911	152.776	154.643	151.326
O−Al−O/(°)	120.536	116.689	115.025	117.906
Al−C/Å	1.963	1.951	1.963	1.953

[a] The period system of MAO nanotube.

It shows the bond distance of Al−O in the nanotube of $[(AlOMe)_3]_{10}$ and $[(AlOMe)_4]_{10}$ is smaller in the end than in the middle. Compared to free cycle chain MAO, bond distances of Al−O is smaller in the nanotube due to formation of π conjugated system. The bond angles of Al−O−Al and O−Al−O in the nanotube of $[(AlOMe)_3]_{10}$ and $[(AlOMe)_4]_{10}$ changes, Al−O−Al increase, and O−Al−O decrease due to bond strength of Al−O being weakened. Bond distances of Al−C are nearly not changed because methyl is only substituent in the wall of the nanotube.

To be continuous, more fused ring MAO have been considered. Naphthalene $[(Al_5O_5)]_n$ and anthracene $[(Al_7O_7)]_n$ formula of MAO and their dimers (Fig.6) are optimized. Naphthalene of MAO has planar cycle structure, while anthracene of MAO has irregular structure in their units. Their dimers have irregular structures and distortion in every layer. They cannot form π conjugated system, so it is difficult to grow nanotube of MAO and it isn't necessary to explore the kind of structures.

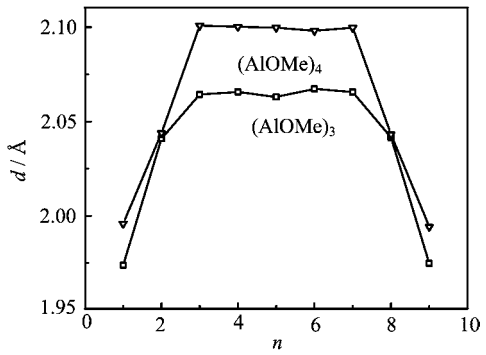

FIG. 5 The average distance d between the cyclic chain structures in the 10 units.

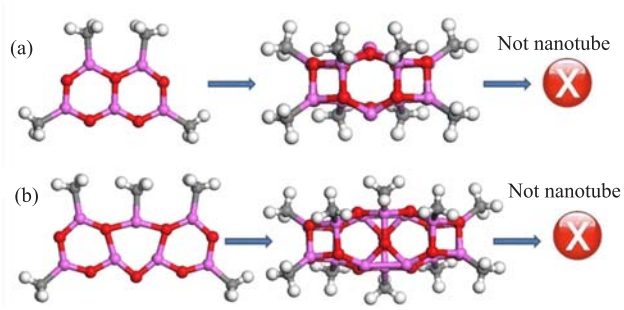

FIG. 6 (a) Naphthalene $[(Al_5O_5)]_n$ and (b) anthracene $[(Al_7O_7)]_n$ formula of MAO.

IV. CONCLUSION

Methylaluminoxane nanotubes derived from cycle chain were optimized by quantum chemical GGA/BLYP methods to determine the preferred structural characteristics and relative stabilities. $[(AlOMe)_3]_n$ and $[(AlOMe)_4]_n$ are preferred. The preference is due to π-electron donation from the lone pairs of oxygen to the vacant p-orbital of aluminum, which cannot be properly achieved by smaller rings. This stability results increase as a function of the size of the nanotube. Long tubes are preferred, owing to the larger proportion of favorable chain rings. To be stable, methylaluminoxane nanotubes need to be longer. Shorter tubes are destabilized due to more unsaturated aluminum and oxygen in the end. Chemical and physical properties of methylaluminoxane nanostructures should differ significantly from their parent carbon analogues, especially due to the high polarity of the Al−O bond. This novel structure of MAO is expected to provide its contribution to the field of polyolefin in the near future.

Supplementary material: The PBD files of the optimized structures are available, including $[(Al_2O_2)]_n$ (n=1−3), $[(Al_3O_3)]_n$ (n=1−10), $[(Al_4O_4)]_n$ (n=1−10), $[(Al_5O_5)]_n$ (n=1, 2), $[(Al_7O_7)]_n$ (n=1, 2).

DOI:10.1063/1674-0068/28/cjcp1412219

[1] H. Sinn, W. Kaminsky, H. J. Vollmer, and R. Woldt, Angew. Chem. Int. Ed. **92**, 396 (1980).
[2] W. Kaminsky, A. Funck, and H. Hähnsen, Dalton Trans. **7**, 8803 (2009).
[3] P. C. Möhring and N. J. Coville, Coord. Chem. Rev. **250**, 18 (2006).
[4] A. Razavi and U. Thewalt, Coord. Chem. Rev. **250**, 155 (2006).
[5] F. M. Andrew and W. C. Geoffrey, J. Am. Chem. Soc. **126**, 16326 (2004).
[6] J. Amir, K. Ilia, G. Sandro, and D. Robbert, Angew. Chem. Int. Ed. **46**, 6119 (2007).
[7] H. Bertrand, B. Cécile, C. Éric, T. Daniel, D. Alain, and C. Henri, Prog. Poly. Sci. **36**, 89 (2011).
[8] E. Y. X. Chen and T. J. Marks, Chem. Rev. **100**, 1391 (2000).
[9] E. Zurek and T. Ziegler, Prog. Polym. Sci. **29**, 107 (2004).
[10] H. Sinn, Macromol. Symp. **97**, 27 (1995).
[11] M. R. Mason, J. M. Smith, S. G. Bott, and A. R. Barron, J. Am. Chem. Soc. **115**, 4971 (1993).
[12] C. J. Harlan, M. R. Mason, and A. R. Barron, Organometallics **13**, 2957 (1994).
[13] E. Zurek and T. Ziegler, Prog. Polym. Sci. **29**, 107 (2004).
[14] S. Pasynkiewicz, Polyhedron **9**, 429 (1990).
[15] E. Zurek, T. K. Woo, T. K. Firman, and T. Ziegler, Inorg. Chem. **40**, 361 (2001).
[16] II. Zakharov, V. A. Zakharov, A. G. Potapov, and G. M. Zhidomirov, Macromol. Theory Simul. **8**, 272 (1999).
[17] II. Zakharov and V. A. Zakharov, Macromol. Theory Simul. **10**, 108 (2001).
[18] V. N. Panchenko, V. A. Zakharov, I. G. Danilova, E. A. Paukshtis, II. Zakharov, V. G. Goncharov, and A. P. Suknev, J. Mol. Catal. A **174**, 107 (2001).
[19] W. E. Clarke, J. Mol. Struct: THEOCHEM **805**, 101 (2007).
[20] M. Linnolahti and T. A. Pakkanen, Inorg. Chem. **43**, 1184 (2004).
[21] M. Linnolahti, T. N. P. Luhtanen, and T. A. Pakkanen, Chem. Eur. J. **10**, 5977 (2004).
[22] B. J. Delley, J. Chem. Phys. **92**, 508 (1992).
[23] B. J. Delley, J. Chem. Phys. **113**, 7756 (2000).
[24] Becke, Phys. Rev. A **38**, 3098 (1988).
[25] C. Lee, W. Yang, and R. G. Parr, Phys. Rev. B **37**, 785 (1998).
[26] S. Pasynkiewicz, Polyhedron **9**, 429 (1990).

DOI:10.1063/1674-0068/28/cjcp1412219